ELSEVIER

Journal of Alloys and Compounds 293–295 (1999) 476–479

Journal of ALLOYS AND COMPOUNDS

Hydrogen in thin epitaxial Nb films

G. Song*, A. Remhof, D. Labergerie, C. Sutter, H. Zabel

Institut für Experimentalphysik, Festkörperphysik, Ruhr-Universität Bochum, D-44780 Bochum, Germany

Abstract

The solubility isotherms of hydrogen in epitaxial Nb(100) films have been determined via in situ X-ray lattice-parameter measurements. The Nb films were grown by molecular-beam epitaxial techniques on R-Al_2O_3 substrates with different thicknesses varying from 34 to 204 nm. Similar to Nb(110) films, the maximum out-of-plane lattice expansion scales inversely with Nb(100) film thickness. Furthermore, the critical temperature T_c for the α-α' phase transition as derived from the solubility isotherms depends strongly on the film thickness. For both orientations we determine similar T_c's but for film thicknesses below 30 nm, T_c in Nb(100) films are higher by about 80 K as compared to Nb(110) films. The influence of finite size scaling and adhesion of the films to the substrates on the solubility isotherms will be discussed.

Keywords: Nb; Nb-film; Thin epitaxial film; Hydrogen absorption/desorption; X-ray scattering isotherms

1. Introduction

Hydrogen in thin metal films is of much current interest because of their tuneable optical [1] and magnetic properties [2,3]. The basic characteristics of hydrogen in metals are described by solubility isotherms from which, in turn, information on the hydrogen–metal and hydrogen–hydrogen interactions are derived. Due to elastic and electronic boundary conditions in thin films, these parameters as well as critical temperatures and phase boundaries are expected to depend on the film thickness. Solubility isotherms are determined by measuring the dissolved H-concentration, c_H, in the metal matrix as a function of the external hydrogen pressure. However, in the case of thin films, determining c_H remains a challenge, since any of the conventional methods applied to bulk metals are not applicable. Therefore, X-ray measurements of the lattice parameter changes remain as the most useful indicator for the hydrogen uptake. The lattice expansion then needs to be converted to hydrogen concentrations by another independent calibration technique, such as the N^{15} nuclear resonance reaction method. In recent X-ray work we have determined in-situ the solubility isotherms for H in Nb(110) films epitaxially grown on Al_2O_3(11.0) substrates [4]. From out-of-plane lattice parameter measurements we inferred a clear thickness dependence of the isotherms and of the critical temperature T_c for the α-α' phase transition. Furthermore, our X-ray measurements reveal a strong correlation of the lattice expansions parallel and perpendicular to the film plane. This is due to a giant adhesion of Nb(110) films to the Al_2O_3(11.0) substrate [5]. For film thicknesses below 5 nm no in-plane expansion takes place, whereas the out-of-plane expansion saturates at a level of 10% for a hydrogen concentration of roughly 70%. For thicker Nb films and beyond a critical stress, a partial in-plane lattice relaxation occurs resulting in a reduced out-of-plane expansion in saturation. Nb films of more than 500 nm thickness approach the bulk behaviour. Obviously the lattice expansions and hydrogen solubility isotherms in thin films depend on the specific boundary conditions, which need to be well understood. Here we report on most recent X-ray scattering experiment results of solubility isotherms in epitaxial Nb(100) films on R-plane Al_2O_3(10.0) substrates. The aim of the research is to understand in more detail the effect of adhesion and film thickness on the shape of the isotherms.

2. Experimental

We have grown single crystalline Nb(100) oriented films by molecular beam epitaxy (MBE) on R-Al_2O_3 substrates. The Nb deposition was carried out in a Riber EVA 32 MBE machine under ultrahigh vacuum (UHV) conditions (base pressure better than 2×10^{-9} Pa) with a working pressure of 10^{-8} Pa. After chemically etching and rinsing

*Corresponding author. Tel.: +49-234-700-4836; fax: +49-234-709-4173.

E-mail address: gang.song@ruhr-uni-bochum.de (G. Song)

0925-8388/99/$ – see front matter
PII: S0925-8388(99)00468-5

in acetone and isopropanol, the substrates were transferred into the UHV system. Final cleaning was achieved by annealing for 10 min at 1100°C. Nb was evaporated with an electron beam gun at a substrate temperature of 900°C using a growth rate of 0.5 Å/s. Afterwards a Pd film of about 5 nm was deposited on the Nb surface, which enhances the catalytic dissociation of hydrogen molecules at the surfaces. At the same time it protects the Nb surface from oxidation. The X-ray experiments were carried out using Mo–$K_{\alpha 1}$ and Cu–K_{α} radiation for measuring the in- and out-of-plane lattice parameter changes, respectively. We used an X-ray furnace for in-situ loading the hydrogen via the gas phase by controlling the gas pressure and sample temperature, as described in more detail in Ref. [4]. In Fig. 1 the small-angle X-ray reflectivity measurements of the Nb(100) films before and after hydrogen loading are shown. The reflectivity scans exhibit low-frequency oscillations due to the thin Pd cap layer and high-frequency oscillations from the Nb film. After finishing a complete solubility cycle, the roughness of the Nb/Pd interface is increased by a factor of 5. The solid lines shown fits to the data points according to the Parratt-formalism for specular reflection [6]. Bragg scans in the radial direction normal to the film plane before and after hydrogen loading are shown in Fig. 2. After sample preparation and before hydrogen loading the lattice parameters d_{200} are 0.1648 nm for the thinnest film and 0.1654 nm for the thickest film, presumably due to strains induced during film deposition. After exposing the samples up to 800 mbar of hydrogen pressure, corresponding to the saturation of the solubility isotherm, and removing the hydrogen step by step, the lattice expansion immediately relaxes back. In the 'hydrogen free' state, the out-of-plane lattice spacing is contracted by about 0.4% as compared to its initial value (Fig. 2 (bottom)). Furthermore, the radial width of the Bragg peaks has substantially increased, indicative for a loss of structural coherence due to the hydrogen loading procedure. Fig. 3 shows rocking scans through the Nb(100) Bragg peak before and after hydrogen loading of the Nb(100) films. Before hydrogen loading the films exhibit a rather broad mosaic distribution of about 1.4° and 0.19° for the 34 nm 204 nm thick films, respectively. This has to be compared to a mosaicity of typically 0.05° for (110) oriented Nb films. After hydrogen loading the coherent structure breaks further down, which usually leads to an increase of the mosaic distribution. However, in our case the mosaicity increases only for the thickest film, whereas for the other two films a reduction of the rocking width is observed. The lattice parameter changes and rocking width have to be understood in the frame of epitaxial strain after growth and strain release during hydrogen uptake. Finally, in Fig. 4 we show the out-of-plane expansions for three different film thicknesses and in each case for three

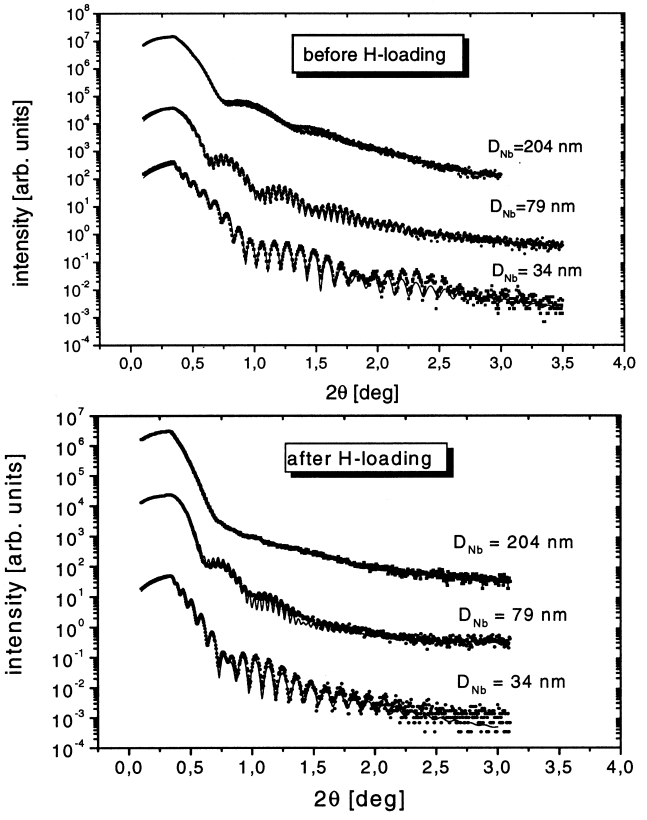

Fig. 1. Small angle X-ray reflectivity measurements of the Nb(100) films with different thicknesses. The narrow oscillations are due to the Nb films, and the wide oscillations to the Pd cap layer. The reflectivity measurements are shown for the sample immediately after growth (top) and after hydrogen uptake to high concentration (bottom).

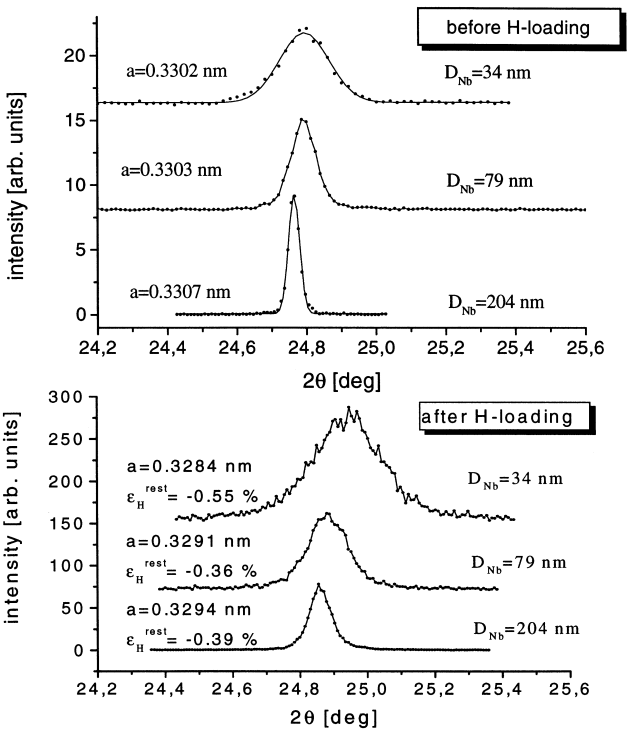

Fig. 2. Bragg scans in the radial direction normal to the film plane of the Nb(100) films.

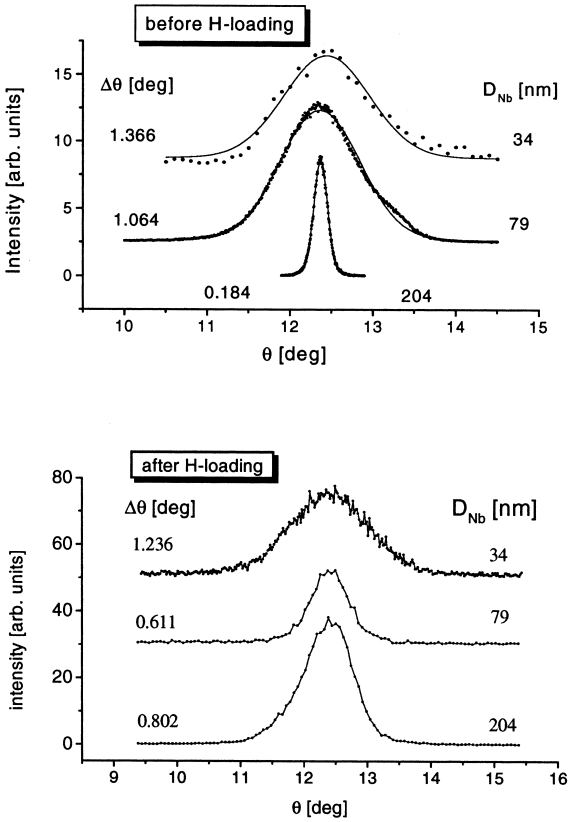

Fig. 3. Rocking scans of the Nb(100) Bragg peaks for different film thicknesses before and after hydrogen loading.

different temperatures. The corresponding in-plane expansions are also shown for the lowest temperature of 473 K. The maximum expansions observed in saturation parallel and perpendicular to the film plane are highly different and the anisotropy clearly depends on the film thickness. The anisotropy is largest for the thinnest film and decreases with increasing film thickness. This behaviour is similar to the Nb(110) films. The solid lines are fits to the data points using an expression for the solubility isotherms described in Ref. [4].

3. Results and discussion

The critical temperature for the α-α′ phase transition in the thin films can be derived using two different approaches. In the first approach we take the slope of the isotherms at the inflection points, which follows the Curie–Weiss law [7]. Fig. 5 (top) shows the extrapolation of T_c from the logarithmic gradients of the isotherms according to the Curie law $(\mathrm{d}(\ln p)/\mathrm{d}\varepsilon_H) \propto (T - T_c)$. In the second approach we estimate T_c from the hydrogen–hydrogen (H–H) interaction energies *u,* as determined by the fits to the measured isotherms, in this case $T_c \propto u \times \varepsilon_{H,max}$, where $\varepsilon_{H,max}$ is the maximum relative lattice parameter change. The T_c's evaluated from the second approach are

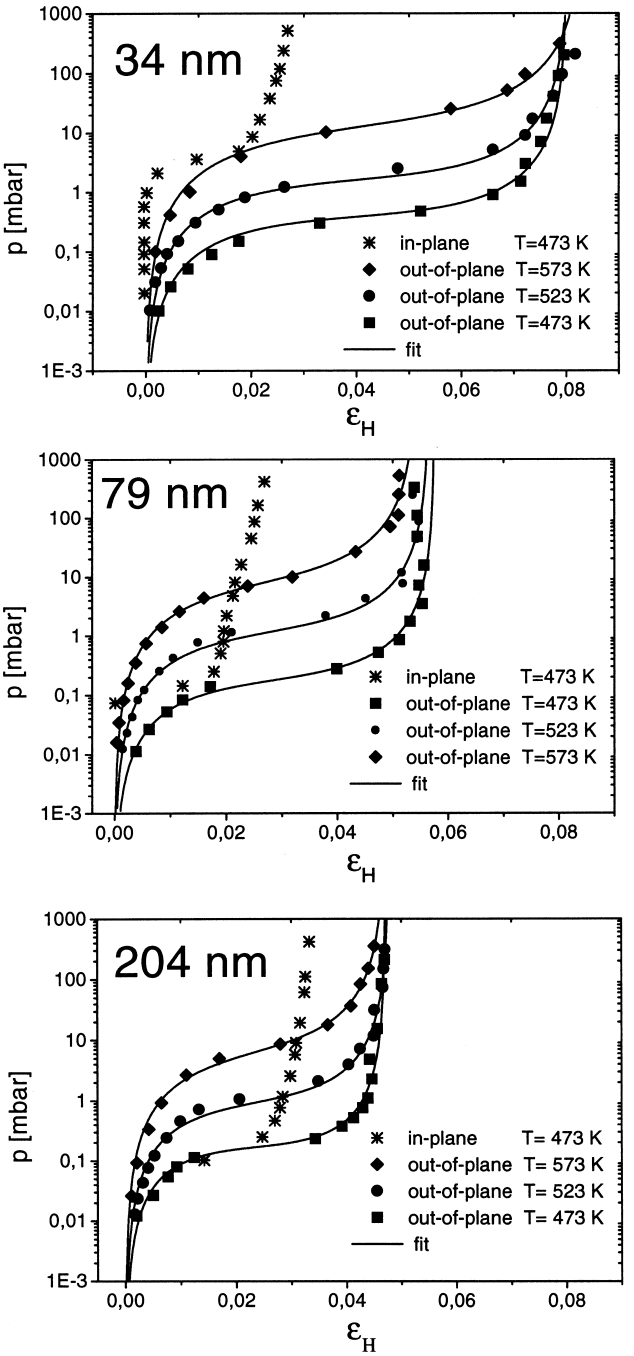

Fig. 4. X-ray measurements of the solubility isotherms for hydrogen in Nb(100) films. p_{h2} is the external hydrogen pressure, and ε_H is the relative lattice parameter change.

plotted as a function of the film thickness in the bottom panel of Fig. 5. The H–H and H–M interactions derived from the solubility isotherms for the 34 nm thick Nb(100) film at $T = 523$ K are respectively 0.09 and 0.16 eV. Comparing these values with the interaction energies derived for the 32 nm thick Nb(110) film [4], the H–H interaction in Nb(100) film is increased by about 20%, whereas the H–M interaction is independent of film thickness and crystal orientation. The increased H–H

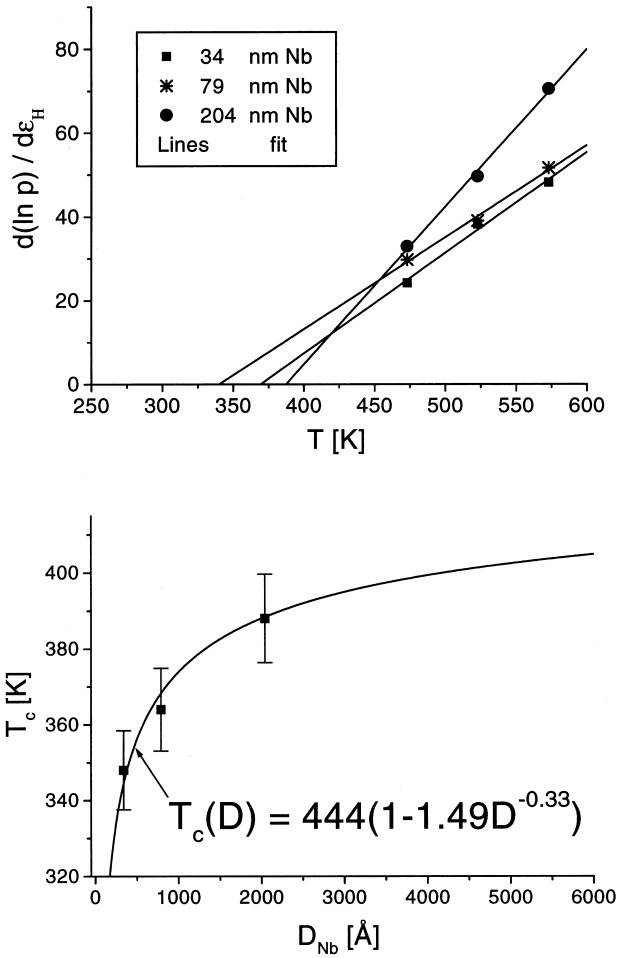

Fig. 5. The slope of the isotherm at the inflection point is plotted as a function of the temperature, showing a Curie–Weiss behaviour (top) and the critical temperatures for the α-α′ phase transition are plotted as a function of the Nb film thickness (bottom).

interaction leads to an enhanced T_c of about 80 K as compared to the 32 nm Nb(110) film. The T_c's evaluated for Nb(100) and Nb(110) films are plotted in Fig. 6. They clearly show a strong dependence on the film thickness. For both orientation the T_c values steadily approach the bulk value for large thicknesses. Finite-size scaling theory predicts a dependence of the critical temperature on the linear dimension of the system according to Ref. [7], $T_c(D) = T_c(\infty)[1 - (D/D_0)^{-\lambda}]$, here λ is the shift exponent, $T_c(\infty) = 444$ K is the critical temperature for bulk Nb, and $T_c(D)$ is the critical temperature for the film of thickness D, with D_0 as a fit parameter. The best fit of the expression to the data points is shown by the solid lines in Fig. 5. From this fit we obtain a shift exponent $\lambda = 0.73$ for Nb(110) films and $\lambda = 0.33$ for Nb(100) films. In both cases the deviation from theoretical predictions ($\lambda = 1.56$

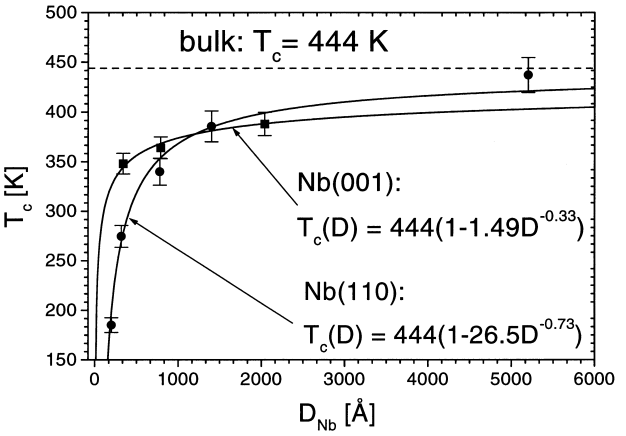

Fig. 6. The critical temperature for the α-α′ phase transition are plotted as a function of the film thickness for both orientations (square (100), circle (110) Nb film).

for the 3D Ising model and 2.0 for the 3D Molecular Field Approximation) is unacceptably large, indicating that finite size scaling may not be the proper description for the present thickness dependence of T_c. The strong anisotropy of hydrogen induced lattice expansion in expitaxial Nb(100) films shows that the adhesion of Nb(100) film on R-Al_2O_3 substrates is large, though it is weaker than that for Nb(110) films. In this case, we infer that the adhesion of the film to the substrates has a bigger effect on the critical temperature than finite size scaling. This is nicely illustrated by the different T_c's for two films of similar thickness, namely 34 nm Nb(100) and 32 nm Nb(110) film, for which we find a difference of about 80 K. In order to separate adhesion from finite size effects, hydrogen solubility isotherms have to be investigated in Nb films, which are either self supporting or deposited on substrates with weak adhesive strength.

References

[1] J.N. Huiberts, R. Griessen, J.H. Rector, R.J. Wijngarten, J.P. Dekker, D.G. de Groot, N.J. Koeman, Nature London 380 (1996) 231.
[2] F. Klose, Ch. Rehm, D. Nagengast, H. Maletta, A. Weidinger, Phys. Rev. Lett. 78 (1997) 1150.
[3] B. Hjörvarsson, J.A. Anderson, P. Isberg, T. Watanabe, T.J. Udovic, G. Andeson, C.F. Majkrzak, Phys. Rev. Lett. 79 (1997) 901.
[4] G. Song, M. Geitz, A. Abromeit, H. Zabel, Phys. Rev. B 54 (1996) 14093.
[5] G. Song, A. Remhof, K. Theis-Bröhl, H. Zabel, Phys. Rev. Lett. 79 (1997) 5062.
[6] L.G. Parratt, Phys. Rev. Lett. 95 (1954) 359.
[7] M.N. Barber, in: C. Domb, J.L. Lebowitz (Eds.), Phase Transitions and Critical Phenomena, Vol. 8, Academic, London, 1983.